

Regiospecificity in the Exchange Coupling of the Spins of Copper(II) Ion Coordinated with the Ring Nitrogen Atoms and *N*-*tert*-Butylaminoxyl Radical Attached as a Substituent on the Pyridine and *N*-Phenylimidazole Rings

Yoichiro Ishimaru,[†] Makoto Kitano,[†] Harumi Kumada,[‡] Noboru Koga,^{*,‡} and Hiizu Iwamura^{*,§}

Department of Chemistry, Graduate School of Science, The University of Tokyo, 7-3-1 Hongo, Bunkyo-ku, Tokyo 113, Japan, and Faculty of Pharmaceutical Science and Institute for Fundamental Research of Organic Chemistry, Kyushu University, Fukuoka 812-82, Japan

Received May 19, 1997

Complexes of bis(hexafluoroacetylacetonato)copper(II) [Cu(hfac)₂] ligated with 3- and 4-(*N*-oxyl-*tert*-butylamino)-pyridines (3NOPy and 4NOPy) and *N*-{3- and 4-(*N*-oxyl-*tert*-butylamino)phenyl}imidazoles (3NOIm and 4NOIm) were prepared. The 1:2 complexes [Cu(hfac)₂(3NOPy and 4NOPy)₂] have hexacoordinated octahedral structures in which the two pyridyl nitrogen atoms are coordinated to the copper(II) ions in the *trans* configuration. The 1:1 complex [Cu(hfac)₂(4NOPy)] has a distorted pentacoordinated pseudo-head-to-tail cyclic dimer structure in which the oxygen atom of the aminoxyl group of one complex is situated at a distance of 2.79 Å from the copper ion of the other complex. The magnetic properties of these and two other complexes, [Cu(hfac)₂(3NOIm and 4NOIm)₂], were investigated using a SQUID susceptometer. Temperature dependence studies of the $\chi_{\text{mol}}T$ values of [Cu(hfac)₂(4NOPy)₂] revealed that the two aminoxyl radicals interact ferromagnetically with the copper(II) ion ($S = 1/2$) with an exchange parameter $J/k_{\text{B}} = 60.4 \pm 3.3$ K to produce a quartet ground state ($S = 3/2$). On the other hand, the $\chi_{\text{mol}}T$ value of the isomeric [Cu(hfac)₂(3NOPy)₂] was nearly constant at 0.5 emu K mol⁻¹ in the temperature range 5–300 K. A rectangular four-spin model was fitted to the $\chi_{\text{mol}}T$ vs T plot for complex [Cu(hfac)₂(4NOPy)] to give $J/k_{\text{B}} = 58.6$ and 58.5 K. Similarly, the J values for [Cu(hfac)₂(3NOIm and 4NOIm)₂] were negative and positive, respectively, but their absolute J values were too small to determine in both cases.

Introduction

Whereas *o*- and *p*-quinodimethanes and their analogues, e.g., the Thiele hydrocarbon, have closed-shell electronic structures, *m*-quinodimethane and the Schlenk hydrocarbon have triplet ground states.¹ The same is true for the corresponding heteroatom-centered diradicals; whereas the *p*-isomer has a quinonediimine *N,N'*-dioxide structure (**p**),^{2a} *m*-phenylenebis(*N*-*tert*-butylaminoxyl) (**m**) is a triplet species in the ground state.^{2b} This regiospecificity in the exchange interaction between the two benzylic radical centers is derived from differences in the phase of the spin polarization of the π -electrons on the benzene ring and has served as an important guiding principle for designing super-high-spin organic molecules as prototypes for purely organic ferromagnets.³ If we are able to assemble unpaired electrons in high concentration by synthesizing super-high-spin molecules with appropriate spatial orientation, then

allow their spins to exchange-couple strongly in two- or three-dimensions in meso- or macroscopic scale, we should be able to obtain molecule-based magnets having reasonably high transition temperatures (T_{C}).⁴

Magnetic metal ions not only have spins of their own right but can also serve as connectors for high dimensional molecular architecture by bridging the lower dimensional organic ligand molecules used as building blocks.⁵ Therefore, heterospin systems consisting of organic free radicals and metal ions constitute one of the most promising design strategies for high T_{C} molecular-based magnets.⁶ Recently we reported successful syntheses of ferri/ferromagnets having two and three *tert*-butylaminoxyl radical units ligated to bis(hexafluoroacetylacetonato)manganese [Mn(hfac)₂].⁷ In these and many previously reported spin systems, the radical centers serve not only as spin sources but also as ligating atoms. Alternatively, the two functions could be separated through space as shown by the

[†] The University of Tokyo.

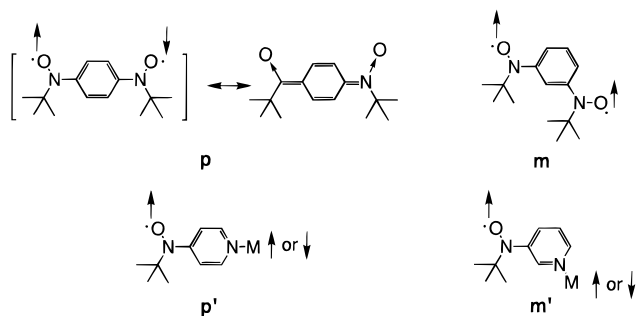
[‡] Faculty of Pharmaceutical Science, Kyushu University.

[§] Institute for Fundamental Research of Organic Chemistry, Kyushu University.

- (1) Platz, M. S. In *Diradicals*; Borden, W. S.; Ed., Wiley: New York, 1982; Chapter 5.
- (2) (a) Nakazono, S.; Koga, N.; Iwamura, H. *Angew. Chem.*, in press. (b) Calder, A.; Forrester, A. R.; James, P. G.; Luckhurst, G. R. *J. Am. Chem. Soc.* **1969**, *91*, 3724. (c) Mukai, K.; Nagai, H.; Ishizu, K. *Bull. Chem. Soc. Jpn.* **1975**, *48*, 2381. (d) Ishida, T.; Iwamura, H. *J. Am. Chem. Soc.* **1991**, *113*, 4238. (e) Kanno, F.; Inoue, K.; Koga, N.; Iwamura, H. *J. Phys. Chem.* **1993**, *97*, 13267.
- (3) (a) McConnell, H. M. *J. Chem. Phys.* **1963**, *39*, 1910. (b) Iwamura, H. *Adv. Phys. Chem.* **1990**, *26*, 179. (c) Dougherty, D. A. *Acc. Chem. Res.* **1991**, *24*, 88. (d) Rajca, A. *Chem. Rev.* **1994**, *94*, 871.

- (4) (a) Kahn, O. *Molecular Magnetism*; VCH Publishers: Weinheim, 1993. (b) Rajca, A. *Chem. Rev.* **1994**, *94*, 871. (c) Gatteschi, D. *Adv. Mater.* **1994**, *6*, 635. (d) Miller, J. S.; Epstein, A. *J. Angew. Chem., Int. Ed. Engl.* **1994**, *33*, 385. (e) Miller, J. S.; Epstein, A. *J. Chem. Eng. News* **1995**, *October 2*, 30. (f) Kahn, O., Ed.; *Magnetism: A Supramolecular Function*; NATO ASI Series C, Kluwer: Dordrecht, 1996. (g) Turnbull, M. M.; Sugimoto, T.; Thompson, L. K., Eds.; *Molecule-based magnetic materials*; ACS Symposium Series 644; American Chemical Society: Washington, DC, 1996. (h) Gatteschi, D. *Curr. Opin. Solid State Mater. Sci.* **1996**, *1*, 192.
- (5) (a) Sauvage, J.-P. *J. Am. Chem. Soc.* **1994**, *116*, 375. (b) Lehn, J.-M. *Supramolecular Chemistry*; VCH Publishers: Weinheim, 1995. (c) Fujita, M.; Ibukuro, F.; Yamaguchi, K.; Ogura, K. *J. Am. Chem. Soc.* **1995**, *117*, 4175. (d) Nierengarten, J.-F.; Dietrich-Buchecker, C. O.; Amabilino, D. B.; Stoddart, J. F. *Chem. Rev.* **1995**, *95*, 2725.

Scheme 1



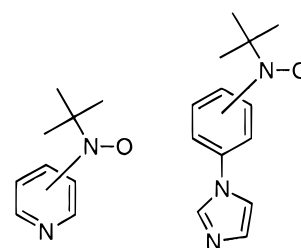
L-S-L system, where L and S are the heteroaromatic ligating site and an unpaired π electron center, respectively. It would then be possible to employ a variety of non-Lewis base free radical ligands other than aminoxyl radicals as bridging units. A successful examples of this is the 1:1 chain polymer complex composed of manganese(II) bis(hexafluoroacetylacetonate) $[\text{Mn}(\text{hfac})_2]$ with di(4-pyridyl)diazomethane in which d^5 Mn(II) is magnetically isolated before irradiation. However, on irradiation the complex becomes a ferrimagnetic chain due to coupling of the 3d-spin of the Mn(II) with the 2p-spin of the carbene centers that arise from by photolysis of the diazo moieties.⁸

To develop such (L-S-L- -M- - -), spin systems, however, it is important to obtain further insight into the magnitude and sign of the exchange coupling between the metal ion and the radical centers. In particular it is of interest to see if the regioselectivity found in organic π -diradicals such as quinodimethanes (**p** vs **m**) is also found for the interaction between free radicals and coordinated magnetic metal ions that are separated by π conjugated ligands (M- -L-S) (**p'** vs **m'** in Scheme 1). Thus, $[\text{Mn}(\text{hfac})_2]$ complexes ligated with either pyridines or *N*-phenylimidazoles having *N*-*tert*-butylaminoxyl radical substituents (NOPy and NOIm, respectively) were deemed to be suitable models and duly prepared. Their magnetic properties revealed that the signs of the exchange interactions between the radical center and the manganese(II) ion for $[\text{Mn}(\text{hfac})_2 \cdot (\text{NOPy})_2]$ and between two manganese(II)

ions for $[\text{Mn}(\text{hfac})_2 \cdot \text{NOIm}]$ dimer were controlled by the regiochemistry of the radical center on the pyridine^{9a} or *N*-phenylimidazole rings.^{9b} Similarly, porphyrinatochromium(III) complex^{9c} ligated with NOPy showed analogous regioselectivity in its magnetic interactions. The observed magnetic properties of the complexes were clearly explained in terms of the spin polarization mechanism³ of the π -electrons.

In metal-radical heterospin systems, the sign and magnitude of the exchange interaction between the two components depends not only on the periodicity of the ligand π orbital, but also strongly on the orbitals occupied by the unpaired d electrons of the metal ion. Both, manganese(II) and chromium(III) have unpaired electrons in the π magnetic orbitals which can overlap with the π orbitals of the ligand. However, as the copper(II) ion has one unpaired electron in the $d_{x^2-y^2}$ orbital that has a σ magnetic character,¹⁰ its complexes are expected to show different magnetic behavior than those of Mn(II) and Cr(III).¹¹

We wish to report here the structural and magnetic characterization of four 1:2 complexes of $\text{Cu}(\text{hfac})_2$ ligated with 3NOPy, 4NOPy, 3NOIm, and 4NOIm and one 1:1 complex of $\text{Cu}(\text{hfac})_2$ with 4NOPy.



3 position : 3NOPy

3NOIm

4 position : 4NOPy

4NOIm

Experimental Section

General Methods. Infrared spectra were recorded on a Hitachi I-5040 FT-IR spectrometer. ¹H NMR spectra were measured on a JEOL 270 Fourier transform spectrometer using CDCl₃ as solvent and referenced to TMS. High-resolution mass spectra (HRMS) were recorded on a JEOL Datum JMS-SX102 spectrometer. Epr spectra were obtained on a Bruker ESP 300 X band spectrometer. Melting points were obtained with a MEL-TEMP heating block and are uncorrected. Elemental analyses were performed in the Analytical Center of this Department.

X-ray Crystal and Molecular Structure Analyses. All the X-ray data were collected using Mo K α radiation on a Rigaku AFC7R four circle diffractometer. Pertinent crystallographic parameters and refinement data are listed in Table 1. The structures were solved in $P\bar{1}$ and $P2_1/n$ for the 1:2 complexes and the 1:1 complex, respectively, by direct methods and refinement converged using the full-matrix least-squares method of the TEXAN Ver. 2.0 program (Molecular Structure Corp.). All non-hydrogen atoms were refined anisotropically; hydrogen atoms were included at standard positions (C-H, 0.96 Å; C-C-H, 109.5, 120, or 180°) and refined isotropically using a rigid model.

Measurements and Analyses of Magnetic Susceptibility. Magnetic susceptibility data were obtained on a Quantum Design MPMS₂

- (6) (a) Eaton, G. R.; Eaton, S. S. *Acc. Chem. Res.* **1988**, *21*, 107. (b) Caneschi, A.; Gatteschi, D.; Laugier, J.; Rey, P.; Sessoli, R. *Inorg. Chem.* **1988**, *27*, 1553. (c) Caneschi, A.; Gatteschi, D.; Renard, J. P.; Rey, P.; Sessoli, R., *Inorg. Chem.* **1989**, *28*, 1976. (d) Caneschi, A.; Gatteschi, D.; Sessoli, R.; Rey, P. *Acc. Chem. Res.* **1989**, *22*, 392. (e) Caneschi, A.; Gatteschi, D.; Rey, P. *Prog. Inorg. Chem.* **1991**, *39*, 331. (f) Burdakov, A. B.; Ovcharenko, V. I.; Ikoriski, V. N.; Pervukhina, N. V.; Podberezskaya, N. V.; Grigor'ev, I. A.; Larionov, S. V.; Volodarsky, L. B. *Inorg. Chem.* **1991**, *30*, 972. (g) Caneschi, A.; Dei, A.; Gatteschi, D. *J. Chem. Soc., Chem. Commun.* **1992**, 630. (h) Caneschi, A.; Chiesi, P.; David, L.; Ferraro, F.; Gatteschi, D.; Sessoli, R. *Inorg. Chem.* **1993**, *32*, 1445. (i) Stumpf, H. O.; Ouahab, L.; Pei, Y.; Grandjean, D.; Kahn, O. *Science* **1993**, *261*, 447. (j) Volodarsky, L. B.; Reznikov, V. A.; Ovcharenko, V. I. *Synthetic Chemistry of Stable Nitroxides*; CRC Press: Boca Raton, FL, 1994; Chapter 4.
- (7) (a) Inoue, K.; Iwamura, H. *J. Am. Chem. Soc.* **1994**, *116*, 3173. (b) Inoue, K.; Iwamura, H. *J. Chem. Soc., Chem. Commun.* **1994**, 2273. (c) Inoue, K.; Iwamura, H. *Synth. Met.* **1995**, *71*, 1791. (d) Inoue, K.; Hayamizu, T.; Iwamura, H. *Mol. Cryst. Liq. Cryst.* **1995**, *273*, 67. (e) Inoue, K.; Hayamizu, T.; Iwamura, H. *Chem. Lett.* **1995**, 745. (f) Mitsumori, T.; Inoue, K.; Koga, N.; Iwamura, H. *J. Am. Chem. Soc.* **1995**, *117*, 2467. (g) Inoue, K.; Hayamizu, T.; Iwamura, H.; Hashizume, D.; Ohashi, Y. *J. Am. Chem. Soc.* **1996**, *118*, 1803. (h) Inoue, K.; Iwamura, H. *Adv. Mater.* **1996**, *8*, 73. (i) Oniciu, D. C.; Matsuda, K.; Iwamura, H. *J. Chem. Soc., Perkin Trans. II* **1996**, 907. (j) Iwamura, H.; Inoue, K.; Hayamizu, T. *Pure Appl. Chem.* **1996**, *68*, 243. (k) Inoue, K.; Iwamura, H. *Mater. Res. Soc. Symp. Proc.* **1996**, *413*, 313.
- (8) (a) Koga, N.; Ishimaru, Y.; Iwamura, H. *Angew. Chem., Int. Ed. Engl.* **1996**, *108*, 802. (b) Koga, N.; Iwamura, H. *Mol. Cryst. Liq. Cryst.* **1997**, *305*, 415.

- (9) (a) Kitano, M.; Ishimaru, Y.; Inoue, K.; Koga, N.; Iwamura, H. *Inorg. Chem.* **1994**, *33*, 6012. (b) Ishimaru, Y.; Inoue, K.; Koga, N.; Iwamura, H. *Chem. Lett.* **1994**, 1693. (c) Kitano, M.; Koga, N.; Iwamura, H. *J. Chem. Soc., Chem. Commun.* **1994**, 447.
- (10) (a) Caneschi, A.; Gatteschi, D.; Sessoli, R.; Rey, P., *Acc. Chem. Res.* **1989**, *22*, 392. (b) Luneau, D.; Rey, P.; Laugier, J.; Fries, P.; Caneschi, A.; Gatteschi, D.; Sessoli, R. *J. Am. Chem. Soc.* **1991**, *113*, 1245.
- (11) (a) Sano, Y.; Tanaka, M.; Koga, N.; Matsuda, K.; Iwamura, H.; Rabu, P.; Drillon, M. *J. Am. Chem. Soc.* **1997**, *119*, 8246. (b) Karasawa, S.; Tanaka, M.; Koga, N.; Iwamura, H. *J. Chem. Soc., Chem. Commun.* **1997**, 1359.

Table 1. Crystallographic Data and Experimental Parameters for Cu(hfac)₂(4NOPy)₂, Cu(hfac)₂(3NOPy)₂, and Cu(hfac)₂(4NOPy)

	Cu(hfac) ₂ (4NOPy) ₂	Cu(hfac) ₂ (3NOPy) ₂	Cu(hfac) ₂ (4NOPy)
empirical formula	C ₂₈ H ₂₈ N ₄ O ₆ F ₁₂ Cu	C ₂₈ H ₂₈ N ₄ O ₆ F ₁₂ Cu	C ₁₉ H ₁₅ N ₂ O ₅ F ₁₂ Cu
<i>a</i> , Å	11.621(5)	11.089(5)	9.571(4)
<i>b</i> , Å	12.602(6)	12.174(3)	19.915(4)
<i>c</i> , Å	6.717(2)	6.519(1)	13.439(5)
α, deg	98.67(3)	94.18(2)	
β, deg	90.98(3)	95.04(3)	96.88(3)
γ, deg	64.36(4)	108.39(2)	
<i>V</i> , Å ³	875.3(7)	827.2(5)	2543(1)
<i>Z</i>	1	1	4
<i>fw</i>	808.08	808.08	642.86
space group	<i>P</i> $\bar{1}$ (No. 2)	<i>P</i> $\bar{1}$ (No. 2)	<i>P</i> 2 ₁ / <i>n</i> (No. 14)
<i>T</i> , °C	20	20	20
λ, Å	0.71069	0.71069	0.71069
ρ _{calc} , g cm ⁻³	1.533	1.622	1.679
μ, cm ⁻¹	7.32	7.75	9.79
<i>R</i> (<i>F</i> ₀) ^a	0.079	0.071	0.078
<i>R</i> _w (<i>F</i> ₀) ^a	0.095	0.099	0.075

$$^a R = \sum ||F_o| - |F_c|| / \sum |F_o|; R_w = [(\sum w(|F_o| - |F_c|)^2) / \sum w F_o^2]^{1/2}.$$

SQUID susceptometer and corrected for the magnetization of the sample holder and capsule, and for diamagnetic contributions to the samples which were estimated from Pascal's constants. Temperature dependence of the molar paramagnetic susceptibility χ_{mol} was expressed by $\chi_{mol}T$ vs T plots and analyzed in terms of models for the magnetic structures determined by X-ray structural analyses or assumed by analogy. Any magnetic interaction due to higher order structures revealed at lower temperatures was treated by assuming a mean-field theory and expressed by the Weiss temperature θ .

Preparation of the Ligands and the Copper Complexes. Unless otherwise stated, preparative reactions were carried out under a high purity dry nitrogen atmosphere. Tetrahydrofuran (THF) and dichloromethane were distilled from sodium benzophenone ketyl and over calcium hydride, respectively. Bis(hexafluoroacetylacetonato)copper(II) [Cu(hfac)₂], 2-methyl-2-nitrosopropane,¹² and 3-(3- and 4-bromophenyl)imidazole¹³ were prepared and purified by the literature procedures. Isomeric pyridine ligands having aminoxyl radical substituents, 4NOPy and 3NOPy, were prepared according to the method reported previously.^{9a}

3-(3-(*N*-tert-Butyl-*N*-hydroxyamino)phenyl)imidazole (3NOHIm). To a solution of 2.2 g (9.9 mmol) of 3-(3-bromophenyl)imidazole in 100 mL of dry THF at -78 °C was added 12.8 mL of a 1.6 M solution of *n*-butyllithium in *n*-hexane. After stirring for 30 min, a solution of 0.85 g (9.9 mmol) of 2-methyl-2-nitrosopropane in 15 mL of THF was added dropwise. The reaction mixture was stirred for 1 h at -78 °C and then left overnight at room temperature. After the usual workup, the resultant brown solid was chromatographed on aluminum oxide with dichloromethane as eluent to give 0.57 g (2.5 mmol, 25.3% yield) of the hydroxyamine as a brown, air-sensitive solid. It was oxidized as described below without further purification.

3-(4-(*N*-tert-Butyl-*N*-hydroxyamino)phenyl)imidazole (4NOHIm). This was prepared using 4-bromophenylimidazole in place of 3-bromophenylimidazole in a manner similar to that used for the preparation of the 3-hydroxyamine derivative. Chromatography on aluminum oxide with dichloromethane as eluent gave the 4-hydroxyamine (23.4% yield) as a white solid, mp 155–158 °C; IR (KBr) ν 3115 cm⁻¹; ¹H NMR (270 MHz, CDCl₃) δ 1.18 (s, 9H), 1.60 (br, 1H), 7.19 (s, 1H), 7.25 (d, *J* = 8.8 Hz, 2H), 7.27 (s, 1H), 7.37 (d, *J* = 9.2 Hz, 2H), 7.82 (s, 1H). Anal. Calcd for C₁₃H₁₇N₃O: C, 67.50; H, 7.42; N, 18.17. Found: C, 67.33; H, 7.37; N, 18.14.

3-(3-(*N*-tert-Butyl-*N*-oxylamino)phenyl)imidazole (3NOIm). To a solution of 0.025 g (0.11 mmol) of 3NOHIm in 20 mL of dry CH₂-

Cl₂ was added 0.33 g of freshly prepared Ag₂O. The suspension was stirred for 120 min and filtered. The resulting orange filtrate was used for metal complexation without further purification. EPR (CH₂Cl₂) *g* = 2.0058, *a*_N = 12.51 G.

3-(4-(*N*-tert-Butyl-*N*-oxylamino)phenyl)imidazole (4NOIm). This radical was prepared in a manner similar to that described for preparation of 3NOIm using 4NOHIm in place of 3NOHIm. EPR (CH₂-Cl₂) *g* = 2.0057, *a*_N = 11.87 G.

Bis{4-(*N*-tert-butyl-*N*-oxyamino)pyridine}bis(hexafluoroacetylacetonato)copper(II) {Cu(hfac)₂(4NOPy)₂. A solution of 0.15 g (0.3 mmol) of anhydrous bis(hexafluoroacetylacetonato)copper(II) in 40 mL of *n*-heptane was heated to reflux for 15 min, cooled to room temperature, and a solution of 4NOPy (0.6 mmol) in 10 mL of CH₂Cl₂ added. The solution was left under a stream of nitrogen gas. Whereupon the product crystallized as green plates. Anal. Calcd for C₂₈H₂₈N₄O₆F₁₂Cu: C, 41.62; H, 3.49; N, 6.93. Found: C, 41.53; H, 3.51; N, 7.23.

Bis{3-(*N*-tert-butyl-*N*-oxyamino)pyridine}bis(hexafluoroacetylacetonato)copper(II) {Cu(hfac)₂(3NOPy)₂. This was prepared in a manner similar to [Cu(hfac)₂(4NOPy)₂] using 3NOPy in place of 4NOPy. Orange needles were obtained. Anal. Calcd for C₂₈H₂₈N₄O₆F₁₂Cu: C, 41.62; H, 3.49; N, 6.93. Found: C, 41.33; H, 3.50; N, 6.89.

3-(*N*-tert-Butyl-*N*-oxyamino)pyridinebis(hexafluoroacetylacetonato)copper(II) {Cu(hfac)₂(4NOPy). This was prepared in a manner similar to [Cu(hfac)₂(4NOPy)₂] by mixing equimolar amounts of Cu(hfac)₂ in CH₂Cl₂ and 4NOPy. Dark green brick crystals were obtained. Anal. Calcd for C₁₉H₁₅N₂O₅F₁₂Cu: C, 36.40; H, 2.42; N, 4.47. Found: C, 36.37; H, 2.54; N, 4.40.

Bis{3-(3-(*N*-tert-butyl-*N*-oxylamino)phenyl)imidazole}bis(hexafluoroacetylacetonato)copper(II) {Cu(hfac)₂(3NOIm)₂. This was prepared in a manner similar to [Cu(hfac)₂(4NOPy)₂] using a CH₂Cl₂ solution of 3NOIm. Reddish brown crystals were obtained. Anal. Calcd for C₃₆H₃₄N₆O₆F₁₂Cu: C, 46.08; H, 3.66; N, 8.96. Found: C, 46.06; H, 3.68; N, 8.81.

Bis{3-(4-(*N*-tert-butyl-*N*-oxylamino)phenyl)imidazole}bis(hexafluoroacetylacetonato)copper(II) {Cu(4NOIm)₂(hfac)₂. This was prepared in a manner similar to Cu(4NOPy)₂(hfac)₂ using a CH₂Cl₂ solution of 4NOIm. Red crystals were obtained. Anal. Calcd for C₃₆H₃₄N₆O₆F₁₂Cu: C, 46.08; H, 3.66; N, 8.96. Found: C, 46.19; H, 3.57; N, 9.05.

Results and Discussion

X-ray Crystal and Molecular Structures. Crystallographic data and experimental parameters for [Cu(hfac)₂(4NOPy)₂] and [Cu(hfac)₂(4NOPy)] are summarized in Table 1. Selected bond lengths and angles are given in Table 2.

(A) [Cu(hfac)₂(4NOPy)₂. As shown in the ORTEP drawing of [Cu(hfac)₂(4NOPy)₂] in Figure 1, two pyridyl nitrogen atoms are coordinated to the copper(II) ion in the *trans* configuration. The copper(II) ion resides in the center of symmetry of a distorted octahedron in which bond lengths are Cu–O(1) = 2.294 Å, Cu–O(2) = 2.036(7) Å, and Cu–N(1) = 2.045(9) Å, and the bond angles between Cu–O(1) and the other ligands are nearly 90° (Table 2). As the elongation axis is through O(1)–Cu–O(1'), this indicates that the lobes of the magnetic orbital *d*_{x²-y², which is orthogonal to the *d*_z orbital of Cu(II) ion, are directed toward the O(2)s of the hfac units and the N(1)s of pyridines. Furthermore, the axis leans toward oxygen atom O(2) by ca. 5°, and this is due to the elongation of the Cu–O(1) bond.}

The lone pair of electrons on the pyridyl nitrogen are slanted slightly away from Cu–N(1) as suggested by the Cu–N(1)–C(8) angle of 175.7°.

A similar distortion in geometry together with an elongation axis through the oxygen atoms of the hfac units and the copper

(12) Stowell, J. C. *J. Org. Chem.* **1971**, *36*, 3055.

(13) Johnson, A. L.; Kauer, J. C.; Sharma, D. C.; Dorfman, R. I. *J. Med. Chem.* **1969**, *12*, 1024.

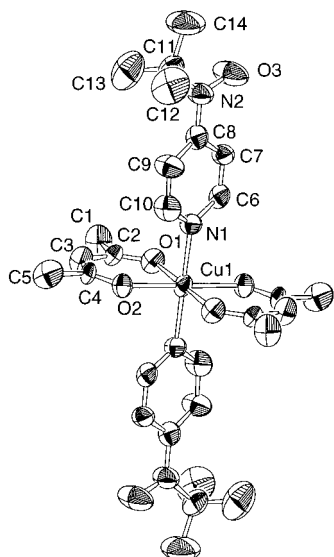


Figure 1. ORTEP drawing showing 30% probability ellipsoids and the atom numbering scheme of the molecular structure for $[\text{Cu}(\text{hfac})_2(4\text{NOPy})_2]$.

Table 2. Selected Bond Lengths (Å) and Angles (deg)

complexes	bond lengths (Å)		bond angles (deg)	
$\text{Cu}(\text{hfac})_2(4\text{NOPy})_2$	Cu—O(1)	2.294(8)	O(1)—Cu—O(2)	95.0(3), 85.0(3)
	Cu—O(2)	2.036(7)	O(2)—Cu—N(1)	89.4(3), 90.6(3)
	Cu—N(1)	2.045(9)	O(1)—Cu—N(1)	88.6(3), 91.4(3)
	N(2)—O(3)	1.28(1)		
	N(2)—C(8)	1.39(1)		
$\text{Cu}(\text{hfac})_2(3\text{NOPy})_2$	Cu—O(1)	2.019(8)	O(1)—Cu—O(2)	95.1(3), 84.9(3)
	Cu—O(2)	2.327(10)	O(2)—Cu—N(1)	92.6(4), 87.4(4)
	Cu—N(1)	2.07(1)	O(1)—Cu—N(1)	90.4(4), 89.6(4)
	N(2)—O(3)	1.29(1)		
	N(2)—C(10)	1.46(1)		
$\text{Cu}(\text{hfac})_2(4\text{NOPy})_2$	Cu—O(1)	1.992(7)	O(1)—Cu—O(2)	94.8(3)
	Cu—O(2)	2.198(7)	O(1)—Cu—O(3)	87.7(3)
	Cu—O(3)	1.933(7)	O(1)—Cu—O(4)	89.4(3)
	Cu—O(4)	1.929(6)	O(1)—Cu—N(1)	162.1(3)
	Cu—N(1)	2.021(8)	O(2)—Cu—O(3)	89.1(3)
	N(2)—O(5)	1.279(9)	O(2)—Cu—O(4)	94.0(3)
			O(2)—Cu—N(1)	103.1(3)
			O(3)—Cu—O(4)	175.9(3)
			O(3)—Cu—N(1)	90.9(3)
			O(4)—Cu—N(1)	90.9(3)

ion was also observed in the analogous 1:2 complex of $\text{Cu}(\text{hfac})_2$ -diazophenyl(4-pyridyl)methane reported previously.^{11a} The dihedral angle between the planes of the *N-tert*-butylaminoxyl moiety and the pyridine ring is 10° , which is larger than the 1.7° angle observed for the corresponding manganese complex $[\text{Mn}(\text{hfac})_2(4\text{NOPy})_2]$.^{9a} The average distance between the radical centers of the neighboring molecules is 5.85 Å in the crystal structure of $[\text{Cu}(\text{hfac})_2(4\text{NOPy})_2]$, and as such the free radical centers may be regarded as well separated.

(B) $[\text{Cu}(\text{hfac})_2(3\text{NOPy})_2]$. As summarized in Table 2, the molecular structure of $[\text{Cu}(\text{hfac})_2(3\text{NOPy})_2]$ is very similar to that of the isomeric 4NOPy complex: two pyridine units are coordinated to the copper ion in a *trans* configuration. As the bond lengths of Cu(II) with the six ligating atoms are 2.019(8), 2.327(10), and 2.07(1) Å for Cu—O(1), Cu—O(2), and Cu—N(1), respectively, the coordination geometry is a distorted octahedral with the O(2)s of hfac units as apical ligands. The dihedral angle between the planes of *N-tert*-butylaminoxyl moiety and the pyridine ring is 39° . In their crystal structures as represented in Figure 2a, both aminoxy groups in $[\text{Cu}(\text{hfac})_2(3\text{NOPy})_2]$ pack in close proximity to those of the neighboring

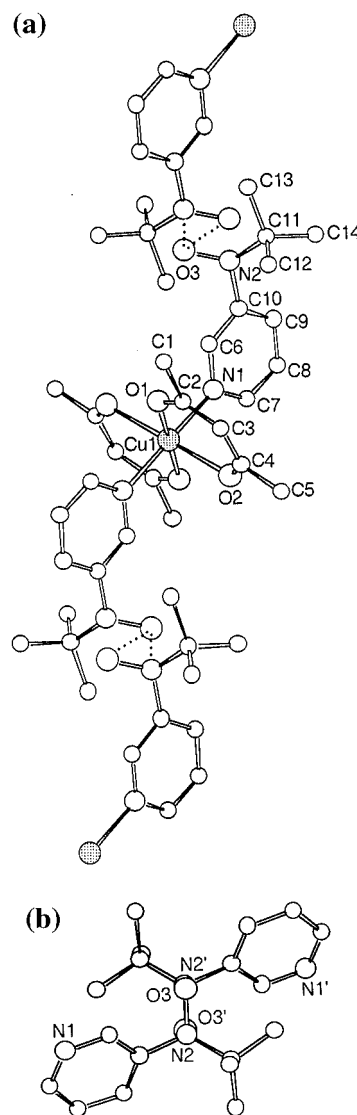


Figure 2. (a) A ball-and-stick model for the crystal structure of $[\text{Cu}(\text{hfac})_2(3\text{NOPy})_2]$ in which the nearest molecules along the *b* axis are presented. Dotted balls and broken lines indicate copper atoms and the distances between the atoms, $r_{\text{O}\cdots\text{O}} = 2.74$ and $r_{\text{N}\cdots\text{O}} = 2.45$ Å, respectively. (b) Molecular arrangement of two pyridylaminoxyl groups projected to the aminoxy radical plane. One N—O of aminoxy unit is shaded.

molecules with a remarkably short distance of 2.45 and 2.74 Å for $\text{N}\cdots\text{O}$ and $\text{O}\cdots\text{O}$ (average distance between the two radical centers is 2.45 Å). This leads to the formation of a magnetically linear chain along the *b* axis. As shown in Figure 2b, the N—O p-orbitals of the adjacent aminoxy radicals overlap each other almost perfectly in a head-to-tail configuration. The observed short intermolecular distance between the aminoxy groups and their relative geometry led us to predict that the crystalline compound would exhibit strongly biased magnetic properties. This is discussed further in the following section.

(C) $[\text{Cu}(\text{hfac})_2(4\text{NOPy})_2]$. The molecular and crystal structure of the 1:1 $[\text{Cu}(\text{hfac})_2(4\text{NOPy})_2]$ complex is shown in Figure 3. The complex has a discrete five-coordinated structure, and the coordination geometry is intermediate between a square pyramid and a trigonal bipyramid. The obtained bond angles of 94.8, 89.1, 94.3, and 103° for O(1)—Cu—O(2), O(3)—Cu—O(2), O(4)—Cu—O(2), and N(1)—Cu—O(2), respectively, indicate that the coordination geometry is closer to a square pyramid than to a trigonal bipyramid in which ideal bond angles

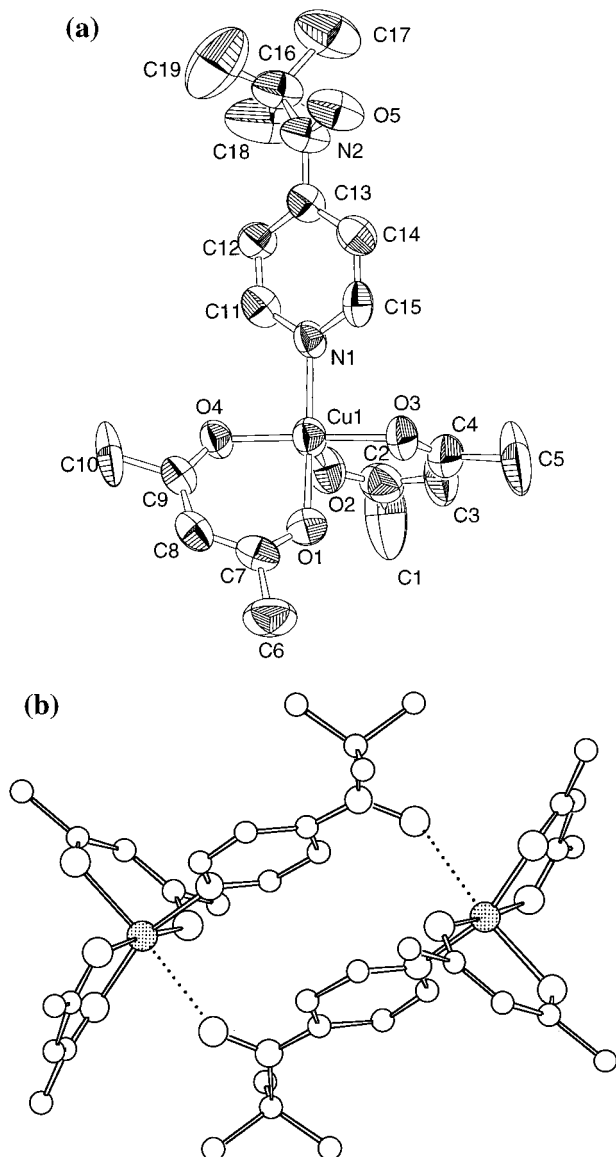


Figure 3. (a) ORTEP drawing showing 30% probability ellipsoids and the atom numbering scheme of the molecular structure and (b) a ball-and-stick model for the dimer structure of $[\text{Cu}(\text{hfac})_2(4\text{NOPy})_2]$. Dotted balls and broken lines indicate copper atoms and the distances between the atoms, $r_{\text{O}-\text{Cu}} = 2.79 \text{ \AA}$, respectively.

are 120° . As the longest bond length between Cu(II) and the five ligating atoms is $2.198(7) \text{ \AA}$ for Cu–O(2), the axial ligand of the square pyramid is considered to be O(2) of the hfac unit. Furthermore, this copper ion interacts with an additional oxygen atom O(5') from the aminoxy group of the neighboring complex. This Cu–O(5') interaction occurs on O(5) at a distance of 2.79 \AA (angle of O(2)–Cu–O(5') = 169°) leading to a pseudo-head-to-tail dimer structure in which two pyridine planes lie in a face-to-face configuration at a distance of $3.76\text{--}3.83 \text{ \AA}$ (Figure 3b). The dihedral angle between the planes of *tert*-butylaminoxy moiety and the pyridine ring is 26° .

Magnetic Properties of $[\text{Cu}(\text{hfac})_2(4\text{NOPy})_2]$, $[\text{Cu}(\text{hfac})_2(3\text{NOPy})_2]$, and $[\text{Cu}(\text{hfac})_2(3\text{NOIm})_2]$. The magnetic susceptibility data of five copper complexes were obtained in the temperature range $2\text{--}300 \text{ K}$ at a constant field of 100 or 800 mT. The temperature dependences of $\chi_{\text{mol}}T$ for $[\text{Cu}(\text{hfac})_2(4\text{NOPy})_2]$ and $[\text{Cu}(\text{hfac})_2(3\text{NOPy})_2]$ are given in Figure 4.

(A) $[\text{Cu}(\text{hfac})_2(4\text{NOPy})_2]$. A $\chi_{\text{mol}}T$ value of $1.29 \text{ emu K mol}^{-1}$ was obtained at 300 K for $[\text{Cu}(\text{hfac})_2(4\text{NOPy})_2]$ and is

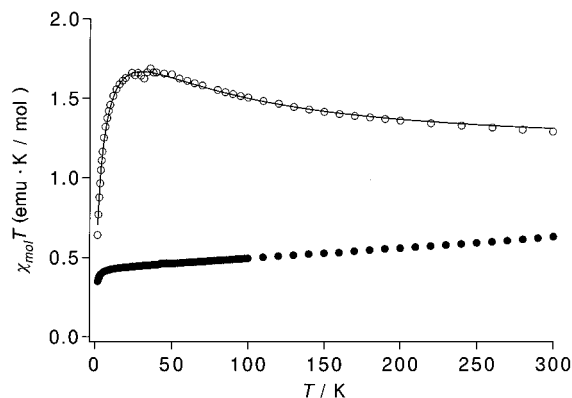


Figure 4. Plots of $\chi_{\text{mol}}T$ vs T for crystalline samples of $[\text{Cu}(\text{hfac})_2(4\text{NOPy})_2]$ (○) and $[\text{Cu}(\text{hfac})_2(3\text{NOPy})_2]$ (●). The solid curve is a theoretical one calculated by eq 1.

close to the theoretical one $\{\chi_{\text{mol}}T = 0.12505 \times g \times 2[3S(S+1)] = 0.12505 \times 2 \times 2 \times (3/2(1/2+1)) = 1.13 \text{ emu K mol}^{-1}$ calculated for three isolated $S = 1/2$ spins in terms of the spin-only equation. As the temperature was decreased, the $\chi_{\text{mol}}T$ value gradually increased, reaching a maximum at 36 K, and rapidly decreasing below 10 K. The maximum $\chi_{\text{mol}}T$ value of $1.69 \text{ emu K mol}^{-1}$ that was observed is slightly smaller than the theoretical one (1.87) calculated for $S = 3/2$. The obtained $\chi_{\text{mol}}T\text{--}T$ curve for $[\text{Cu}(\text{hfac})_2(4\text{NOPy})_2]$ was analyzed quantitatively on the basis of a linear three-spin model $\{S_1\text{--}S_2\text{--}S_3; H = -2J(S_1S_2 + S_1S_3 + S_2S_3)\}$ that was deemed to be appropriate from X-ray molecular and crystal structure analysis. Equation 1 for three spins with $S_1 = S_2 = S_3 = 1/2$ was applied and fitted to the observed $\chi_{\text{mol}}T\text{--}T$ plot for $[\text{Cu}(\text{hfac})_2(4\text{NOPy})_2]$ by means of a least-squares method. All the symbols have their

$$\chi_{\text{mol}}T = \frac{N\mu_B^2 g^2 T}{3k_B(T - \theta)} \frac{6 \exp(3J/T) + 6 \exp(2J/T) + 6}{4(4 \exp(3J/T) + 2 \exp(2J/T) + 2)} \quad (1)$$

usual meaning. The best parameters of best fit were $60.4 \pm 3.3 \text{ K}$, 2.048 ± 0.0091 , $-3.58 \pm 0.09 \text{ K}$ for J/k_B , g , and θ , respectively, and the theoretical curve is represented by a solid line in Figure 4.

(B) $[\text{Cu}(\text{hfac})_2(3\text{NOPy})_2]$. The $\chi_{\text{mol}}T\text{--}T$ plot for the isomeric complex $[\text{Cu}(\text{hfac})_2(3\text{NOPy})_2]$ showed quite different temperature dependence behavior. The $\chi_{\text{mol}}T$ value was ca. $0.6 \text{ emu K mol}^{-1}$ at 300 K and gradually decreased to 0.43 at 10 K, as the temperature was lowered from 300 K. Since the theoretical $\chi_{\text{mol}}T$ values calculated for spin only situations with $S = 1/2$, $3/2$, and with degenerate two doublet and one quartet states are 0.37 , 1.88 , and $1.13 \text{ emu K mol}^{-1}$, respectively, the observed values at 10 and at even 300 K are close to a theoretical ones calculated for $S = 1/2$. There are two possibilities available to explain the observed $\chi_{\text{mol}}T\text{--}T$ plot: (1) The two aminoxy radicals recombined chemically to a diamagnetic dimer¹⁴ during the crystallization. (2) The two spins of the aminoxy radicals canceled each other out by a strong antiferromagnetic interaction. If this is the case, the recombination–dissociation process must be reversible as typical EPR signals due to the aminoxy radical were observed after dissolving the sample in dichloromethane. Possibility (2) was supported by the X-ray analysis of the crystal and the molecular structure of $[\text{Cu}(\text{hfac})_2(3\text{NOPy})_2]$.

(14) Patai, S., Rappaport, Z., Eds.; *Nitrons, nitronates, and nitroxides*; John Wiley & Sons: Chichester, 1989; Chapter 4, p 346.

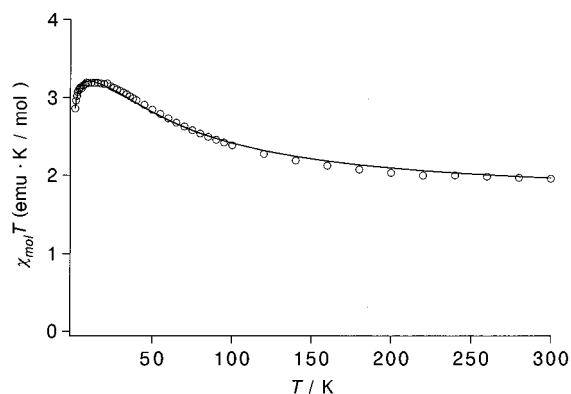
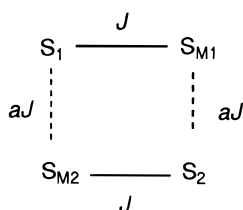


Figure 5. Plot of $\chi_{\text{mol}}T$ vs T for a crystalline sample of $[\text{Cu}(\text{hfac})_2(4\text{NOPy})_2]$. The solid curve is a theoretical one calculated by eq 2.

Scheme 2



The relatively large dihedral angle (39°) between the plane of *N*-*tert*-butylaminoxyl moiety and the pyridine ring is considered to weaken the interaction between the aminoxyl and the copper ion whereas the short distance of 2.45 Å between one aminoxyl group and another one belonging to its nearest neighbor molecule strengthens the through-space antiferromagnetic interaction between the two aminoxyl groups. Recently, we found strong intermolecular antiferromagnetic interactions with $J/k_B = -158$ and -239 K in nitronylnitroxide (**NN**) and iminylnitroxide (**IN**) imidazole derivatives, respectively, in which the relative geometry of the p-orbitals between two aminoxyl radical centers were ideal for overlap; these centers were separated by a short distance of 3.49 and 3.54 Å.¹⁵ As represented in Figure 2b, the observed geometry of the two aminoxyl radical centers in this work was closer to ideal than for the imidazole derivatives. Therefore, their interaction in $[\text{Cu}(\text{hfac})_2(3\text{NOPy})_2]$ is predicted to be extremely strongly antiferromagnetic. If we take the dihedral angle of 39° , the relative geometry of the p-orbitals, and the distance of 2.45 Å into account, $-J_{\text{inter}}$ should be smaller than -239 K ($-J_{\text{intra}} \gg -J_{\text{inter}}$). Therefore, in the $\chi_{\text{mol}}T-T$ plot it appears as if the copper complex has no aminoxyl radical units.

(C) $[\text{Cu}(\text{hfac})_2(4\text{NOPy})_2]$. A plot of $\chi_{\text{mol}}T-T$ for the 1:1 complex is shown in Figure 5. When the temperature was decreased from 300 to 2 K, the $\chi_{\text{mol}}T$ values ($1.96 \text{ emu K mol}^{-1}$ at 300 K) increased gradually, reached a maximum ($3.20 \text{ emu K mol}^{-1}$ at 9 K), and then decreased.

For quantitative analysis of the observed $\chi_{\text{mol}}T-T$ plot in Figure 5, a rectangular four-spin model (Scheme 2) suggested by the X-ray crystal and molecular structure analysis was assumed.

The spin Hamiltonian for such a system is given by $H = -2J(S_1S_{M1} + S_{M2}S_2) - 2aJ(S_1S_{M2} + S_{M1}S_2)$, where J and aJ are intra- and intermolecular exchange coupling parameters,

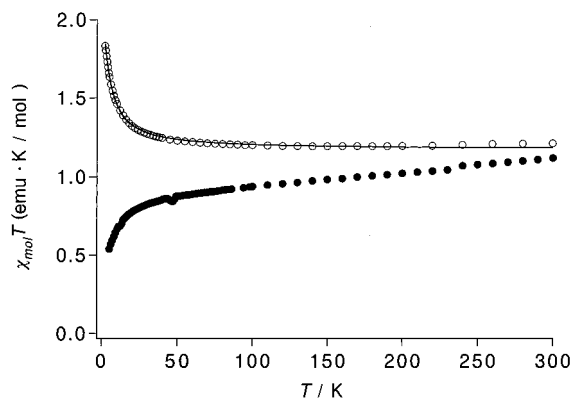


Figure 6. Plots of $\chi_{\text{mol}}T$ vs T for crystalline samples of $[\text{Cu}(\text{hfac})_2(4\text{NOIm})_2]$ (○) and $[\text{Cu}(\text{hfac})_2(3\text{NOIm})_2]$ (●). The solid curve is a theoretical one calculated by eq 1.

respectively. The temperature dependence of the $\chi_{\text{mol}}T$ is then given by eq 2:

$$\chi_{\text{mol}}T = \frac{N\mu_B^2 g^2 T}{3k_B(T - \theta)} \frac{8(a_3 + a_4 + a_5) + 24a_6}{4(a_1 + a_2 + a_3 + a_4 + a_5 + a_6)} \quad (2)$$

$$a_1 = \exp[-(2 + 2a + 2\sqrt{a^2 + a + 1})J/T]$$

$$a_2 = \exp[-(2 + 2a - 2\sqrt{a^2 + a + 1})J/T]$$

$$a_3 = \exp[-(2a + 2)J/T]$$

$$a_4 = \exp(-2aJ/T)$$

$$a_5 = \exp(-2J/T)$$

$$a_6 = 5$$

where all symbols have their usual meaning. Fitting of eq 2 to the observed values was refined by means of a least-squares method. The theoretical curve of the best fit is represented in Figure 5 by a solid line and its parameters, J , a , g , and θ are 58.5 K, 1.001, 2.113, and -0.33 K, respectively. The a value is almost 1, indicating that the magnitude of the exchange interaction of the aminoxyl radical and the copper ion through the pyridine ring and through space are accidentally equal. Although the dihedral angle between the radical plane and pyridine ring is slightly larger (26°), the J/k_B value (58 K) is close to the value of 62 K obtained in $[\text{Cu}(\text{hfac})_2(4\text{NOPy})_2]$ under similar conditions and which is due to the interaction through the pyridine ring.

(D) $[\text{Cu}(\text{hfac})_2(3\text{- and }4\text{NOIm})_2]$. The temperature dependence of $\chi_{\text{mol}}T$ for powder samples of both isomeric 1:2 complexes, $[\text{Cu}(\text{hfac})_2(3\text{NOIm and }4\text{NOIm})_2]$, are shown in Figure 6.

The obtained $\chi_{\text{mol}}T$ values at 300 K for both isomeric copper complexes are close to each other; 1.21 and $1.12 \text{ emu K mol}^{-1}$ for $[\text{Cu}(\text{hfac})_2(3\text{NOIm and }4\text{NOIm})_2]$, respectively, and in good agreement with the theoretical one ($\chi_{\text{mol}}T = 1.13 \text{ emu K mol}^{-1}$) for an isolated three spins system with $S = 1/2$. However, their $\chi_{\text{mol}}T-T$ plots (Figure 6) contrast sharply, especially in the low-temperature region below 30 K. As the temperature was decreased, the $\chi_{\text{mol}}T$ value for $[\text{Cu}(\text{hfac})_2(4\text{NOIm})_2]$ remained nearly constant until 30 K and then increased below this temperature, while the $\chi_{\text{mol}}T$ value for $[\text{Cu}(\text{hfac})_2(3\text{NOIm})_2]$ decreased gradually below 30 K. Although structural informa-

(15) Akabane, R.; Tanaka, M.; Matsuo, K.; Koga, N.; Matsuda, K.; Iwamura, H. *J. Org. Chem.* **1997**, *62*, 8854.

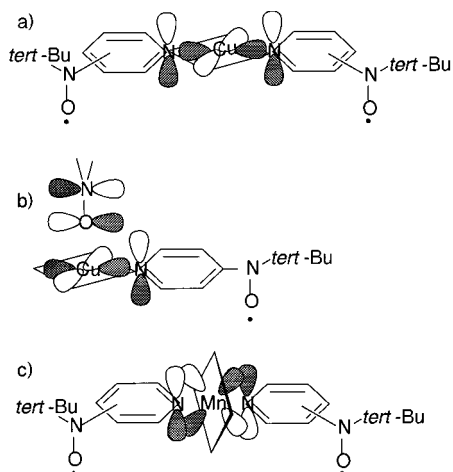


Figure 7. Scheme illustrating the interaction of the magnetic orbital of the copper(II) ion with (a) the π -orbitals at the nitrogen of pyridine ring in the 1:2 complex, (b) the π -orbitals of pyridine and aminoxyl radical in the 1:1 dimer complex. The interaction scheme for the manganese(II) complex is depicted in (c).

tion by X-ray analysis for both complexes are missing, a linear three-spin model was assumed and the observed $\chi_{\text{mol}}T-T$ plots were fitted to eq 1. The best-fit parameters were $J/k_B = 4.26 \pm 0.08$ K, $\theta = -0.024 \pm 0.008$ K, and $g = 2.043 \pm 0.002$, for $[\text{Cu}(\text{hfac})_2(4\text{NOIm})_2]$. These values suggest a weak ferromagnetic interaction is operating between the copper ion and aminoxyl radical in $[\text{Cu}(\text{hfac})_2(4\text{NOIm})_2]$. Antiferromagnetic interactions were expected to take place between these centers in $[\text{Cu}(\text{hfac})_2(3\text{NOIm})_2]$ but the obtained J value (-2.74 K) is too small to discuss its magnitude.

Ferromagnetic Exchange Interaction in the Copper Complexes and Comparison of Its Interaction with That in the Corresponding Manganese Complexes. The magnetic interactions between copper(II) and *N*-(4-pyridyl)-*N*-*tert*-butylaminoxyl radical found in this work are unique in that they are ferromagnetic and considerably large in magnitude: $J/k_B = 60.4$ and 58.5 K for the 1:2 and 1:1 complexes, respectively. The couplings of the copper ions attached directly to the aminoxyl radicals via their oxygen atoms are well documented and typically antiferromagnetic due to the overlap of the singly occupied orbitals of the metal ion and the free radical. Only when the oxygen atom of an aminoxyl radical is axially bound to a tetragonal copper (II) ion, a weak ferromagnetic coupling (~ 20 K) develops.¹⁰ The relative geometry between the magnetic orbital of the copper(II) ion and the p-orbital of the pyridine ring as revealed by X-ray molecular structure analyses is illustrated in Figure 7.

The magnetic orbital $d_{x^2-y^2}$, orthogonal to the elongated axis of octahedral Cu(II), is directed to the two nitrogen atoms of the pyridine groups and the oxygen atoms of the two hfac ligands in the 1:2 complexes (Figure 7a). On the other hand, the magnetic orbital $d_{x^2-y^2}$ of Cu(II) on the basal plane of the square pyramid is directed to one pyridyl nitrogen atom and three of the oxygen atoms of the hfac units in the 1:1 complex. Furthermore, the oxygen atom of the aminoxyl radical in the other molecule of the dimer is situated at the axial position of the pentacoordinated structure (Figure 7b). As seen clearly in Figure 7, both the magnetic orbital $d_{x^2-y^2}$ of Cu(II) and the π -orbital at the nitrogen atom of the pyridine unit or the oxygen atom in the aminoxyl radical unit have no significant overlap and the relative geometry between them should be orthogonal. This orthogonality of the singly occupied d orbital and nitrogen 2p-orbital to which spin is polarized via the π -electrons on the

pyridine ring from the aminoxyl radical center is responsible for the ferromagnetic interaction. For the construction of super-high-spin molecules in hetero-spin systems, this consideration lead to the interesting and useful conclusion that copper(II) ion in normal 5- and 6-coordination induces parallel spin on the ligating atom of conjugated π -ligands such as pyridine, as illustrated in this work. There is one important precedent for such ferromagnetic coupling in the copper(II) complex with 2-(2-pyridyl)-4,4,5,5-tetramethyl-4,5-dihydro-1*H*-imidazolyl-1-oxyl in which both the imino and pyridyl nitrogens are attached to the copper ion as a bidentate ligand and the ferromagnetic coupling is as strong as >215 K.^{10b} In this case, delocalization of the spin by the contribution of an aminyl nitrone resonance hybrid and proximity of the imino nitrogen atom with respect to the aminoxyl radical center, which facilitate the spin polarization at the imino nitrogen, appear to be responsible for the stronger ferromagnetic coupling.

When the molecular structure (Figure 1) of $[\text{Cu}(\text{hfac})_2(4\text{NOPy})_2]$ found in this work is compared with those of the corresponding manganese complexes, e.g. $[\text{Mn}(\text{hfac})_2(4\text{NOPy})_2]$, reported previously,^{9a} we note that both the complexes have similar molecular structures in which nitrogen atoms of two 4NOPys are coordinated to the metal ion in the *trans* configuration. However, when the J/k_B values of both the complexes are compared, the signs are opposite: positive for the former and negative for the latter with $J/k_B = 60.4$ and -12.4 K for $[\text{Cu}(\text{hfac})_2(4\text{NOPy})_2]$ and $[\text{Mn}(\text{hfac})_2(4\text{NOPy})_2]$, respectively. Furthermore, we note that the magnitude for the copper(II) ion is about five times larger than the one for the manganese complex. The torsion angles between the *N*-*tert*-butylaminoxyl and the pyridine ring are 10 and 1.7° for $[\text{Cu}(\text{hfac})_2(4\text{NOPy})_2]$ and $[\text{Mn}(\text{hfac})_2(4\text{NOPy})_2]$, respectively, and thus does not explain the difference. Therefore the difference in the J/k_B values between the copper and the manganese complexes is considered to be derived from the magnetic d orbitals occupied by the unpaired electrons in the metal ions, $d_{x^2-y^2}$ for copper(II) and d_{xy} , d_{yz} , d_{xz} , $d_{x^2-y^2}$, and d_{z^2} for manganese(II) ions. The coordination geometry of the $[\text{Mn}(\text{hfac})_2(4\text{NOPy})_2]$ complex was a slightly elongated octahedron in which the axial ligands are the nitrogen atoms of pyridine groups. Therefore, the magnetic orbitals of manganese(II) ion can overlap with the π orbital at the nitrogen on the pyridine ring (Figure 7c) to produce an antiferromagnetic interaction with the spin on nitrogen transmitted in the same way as the case for the copper complex.

The temperature independent $\chi_{\text{mol}}T$ value for $[\text{Cu}(\text{hfac})_2(3\text{NOPy})_2]$ was also observed in the $\chi_{\text{mol}}T-T$ plot for $[\text{Mn}(\text{hfac})_2(3\text{NOPy})_2]$ under similar conditions. As reported previously,^{9a} its magnetic interaction could not be explained completely due to a lack of structural information. Present work on $[\text{Cu}(\text{hfac})_2(3\text{NOPy})_2]$ suggests that $[\text{Mn}(\text{hfac})_2(3\text{NOPy})_2]$ might have an analogous crystal structure and that its magnetic property is controlled by the same intermolecular antiferromagnetic interactions as discussed in the case of $[\text{Cu}(\text{hfac})_2(3\text{NOPy})_2]$.

Conclusion

The magnetic properties of isomeric complexes $[\text{Cu}(\text{hfac})_2(3\text{NOPy})_2]$ and $[\text{Cu}(\text{hfac})_2(4\text{NOPy})_2]$ are in stark contrast, although both complexes had similar molecular structures in which the two NOPys were ligated to one copper ion in the *trans* configuration. In $[\text{Cu}(\text{hfac})_2(4\text{NOPy})_2]$, two aminoxyl radicals interact ferromagnetically with the copper ion via the π conjugated pyridyl ring to produce a ground-state quartet species. The J/k_B value between the copper ion and the aminoxyl radical was estimated

to be 60.4 ± 3.34 K by fitting a linear three-spin model to the observed $\chi_{\text{mol}}T-T$ curve. On the other hand, the $\chi_{\text{mol}}T-T$ plot showed a horizontal line of height 0.6–0.4 emu K mol⁻¹ in the [Cu(hfac)₂(3NOPy)₂] complex, suggesting that only the spin of the isolated copper ion remained and those of the two aminoxy radicals canceled each other out by strong antiferromagnetic intermolecular interactions between the nearest neighbor molecules (Figure 2b). The 1:1 complex, [Cu(hfac)₂(4NOPy)], has a pseudocyclic dimer structure in which the aminoxy radical and the copper ion interact ferromagnetically both through bond and through space with $J/k_B = 58.6$ and 58.5 K. In the NOIm–Cu systems, similar magnetic behaviors were observed but the magnitude of interaction was much smaller; J/k_B for [Cu(hfac)₂(4NOIm)₂] is 4.26 ± 0.08 K.

The weak ferro- and presumably antiferromagnetic interactions between the copper ion and the aminoxy radical in [Cu(hfac)₂(4NOIm and 3NOIm)₂], respectively, are ascribed to the weakened through-bond exchange coupling due to the presence of many intervening π bonds.

It is in line with the conclusion of this work that chain polymer complexes made of Mn(hfac)₂ and Cu(hfac)₂ with di-(4-pyridyl)diazomethane gave dilute paramagnets due to Mn(II) and Cu(II) ions, respectively, which became ferri- and ferromagnetic chains of considerable correlation length after photolysis of the diazo moieties to generate triplet carbene centers.^{8,11}

Acknowledgment. This work was supported by a Grant-in-Aid for COE Research “Design and Control of Advanced Molecular Assembly Systems” from the Ministry of Education, Science and Culture, Japan (#08CE2005).

Supporting Information Available: Tables SI–SXI, SVII–SXII, and SXIII–SXVIII, listing experimental details, atomic coordinates, and isotropic thermal factors, anisotropic displacement parameters, bond lengths, bond angles, and torsion angles for [Cu(hfac)₂(3NOPy and 4NOPy)₂] and [Cu(hfac)₂(4NOPy)], respectively, are available (80 pages). Ordering information is given on any current masthead page.

IC970602S